Available online at www.sciencedirect.com
ScienceDirect
Journal of the European Ceramic Society 31 (2011) 569–576
www.elsevier.com/locate/jeurceramsoc

Microstructure and piezoelectric properties of CuO added (K, Na, Li)NbO_3 lead-free piezoelectric ceramics

F. Azough, M. Wegrzyn, R. Freer*, S. Sharma, D. Hall

Materials Science Centre, School of Materials, University of Manchester, Grosvenor Street, Manchester, M1 7HS, UK

Received 16 April 2010; received in revised form 16 October 2010; accepted 30 October 2010
Available online 19 November 2010

Abstract

Lead-free $Na_{0.5}K_{0.5}NbO_3$ (NKN) and $Na_{0.475}K_{0.475}Li_{0.05}NbO_3$ (NKLN) ceramics doped with CuO were prepared by the mixed oxide route. The powders were calcined at 850–930 °C and sintered at 850–1100 °C. Small additions of CuO reduced the sintering temperature and increased the density to 96% theoretical. Cu first appears to enter the A site then the B site. In NKLN the orthorhombic–tetragonal and tetragonal–cubic phase transitions are approximately 150 °C lower and 50 °C higher, respectively than in NKN. With increasing addition of Cu to NKN and NKLN the remanent polarization (P_r) increased and coercive field (E_c) decreased. NKLN prepared with 0.4 wt% CuO exhibited a saturation polarization (P_{sat}) of 30 μC/cm^2, remanent polarization (P_r) of 27 μC/cm^2 and coercive field (E_c) of 1.0 kV/mm. CuO caused the NKLN ceramics to harden considerably; the mechanical quality factor (Q_m) increased from 50 to 260, $d_{33} \sim 285$ and piezoelectric coupling factors were >0.4.

Keywords: Perovskites; Piezoelectric properties; Electron microscopy

1. Introduction

Lead-based piezoelectric ceramics have been an industry standard for many decades and are widely used in actuators, sensors, and transducers because of their excellent electrical properties.[1] However, there is growing environmental concern about the use of lead in such products and the EU has already introduced legislation to restrict the use of a range of hazardous substances which is directly relevant to the piezoelectrics.[2] As a consequence there has been much activity to find and develop lead-free electroceramics with comparable piezoelectric properties to the lead containing ceramics. Alkali niobates, based on sodium potassium niobate, $Na_{0.5}K_{0.5}NbO_3$ (NKN) have emerged as one of the most promising candidates as lead-free piezoelectric ceramics because of their strong ferroelectricity and high Curie temperature.[3] The piezoelectric properties of NKN ceramics have been further improved for practical applications by formation of solid solutions with $LiNbO_3$,[4] $LiTaO_3$,[5] $LiSbO_3$,[6] $CaTiO_3$,[7] $SrTiO_3$,[8] $BiScO_3$,[9] $BiFeO_3$[10] and $BaTiO_3$.[11] In seeking solid solution formation, part of the drive has been to develop morphotropic phase boundaries (MBP), where optimum piezoelectric properties have been obtained in the traditional $PbZrO_3$–$PbTiO_3$ (PZT) system.[1]

With the high volatility of sodium and potassium compounds above 800 °C it is difficult to obtain high density NKN ceramics using conventional fabrication processes. To overcome such limitations alternative approaches have been explored including hot-pressing,[11] high energy milling,[13] and spark plasma sintering.[14] A prime requirement for the miniaturisation in many systems is a low sintering temperature, and this is particularly true for multilayered structures where silver is the intended electrode material.[15] Sintering aids such as ZnO,[15] CuO,[16,17] V_2O_5,[18] MnO_2[19] have also been employed to improve the sinterability of NKN ceramics. CuO is now established as an effective sintering aid for NKN-based ceramics, enabling liquid phase sintering at temperatures around 960 °C and able to modify the microstructure and piezoelectric properties.[16,17] To achieve even lower sintering temperatures (~900 °C), CuO has been used in conjunction with ZnO.[15]

Compounding NKN with other perovskite structure phases frequently yields enhanced properties. Saito et al.[20] demonstrated that in the systems NKN–$LiTaO_3$ and NKN–$LiTaO_3$–$LiSbO_3$ piezoelectric properties approaching those of PZT could be obtained near the MBP. Similarly,

* Corresponding author. Tel.: +44 161 306 3564; fax: +44 161 306 8877.
E-mail address: Robert.Freer@manchester.ac.uk (R. Freer).

0955-2219/$ – see front matter © 2010 Elsevier Ltd. All rights reserved.
doi:10.1016/j.jeurceramsoc.2010.10.033

combining NKN with mixed lithium Ta/Nb perovskites[21] or simply $LiNbO_3$[4] yields very encouraging properties. In the latter case NKN–$LiNbO_3$ (or NKLN) ceramics have exhibited high d_{33} values around 230 pC/N.[22] In the present study NKN and NKLN ceramics (with additions of CuO) prepared by the mixed oxide route were investigated. The NKLN composition selected was NKN + 5 mole% $LiNbO_3$ on the basis of its high d_{33} values.[22] The primary objective was to understand the role of CuO additions on the sintering behaviour, microstructure and properties of NKLN ceramics. Direct comparison is made to the properties of the base material NKN to highlight the effect of Li in the structure.

2. Experimental

$Na_{0.5}K_{0.5}NbO_3$ (NKN) and $Na_{0.475}K_{0.475}Li_{0.05}NbO_3$ (NKLN) ceramics were prepared by the conventional mixed oxide route. The starting materials were high purity metal oxide or carbonate powders, Nb_2O_5 (>99.9%), K_2CO_3 (>99.8%), Na_2CO_3 (>99.8%), Li_2CO_3 (>99.99%), and CuO (>99.9%). The carbonates were dried at 250 °C for 6 h prior to use, then all the powders were weighed according to the required compositions and mixed for 24 h using propan-2-ol and zirconia media. The powders were calcined at 850–930 °C for 4 h then CuO (0.075–0.8 wt%) was added, wet milled for 24–48 h and dried. Pellets were prepared by pressing powders in a 10 mm diameter die at 100 MPa, then sintering at 850 °C to 1100 °C for 2–18 h and finally cooling to room temperature at 180 °C/h.

Product densities were determined from weight and dimension measurements. The crystal structures were examined by X-ray diffraction. This was undertaken using a Philips Analytical, X'pert-MPD, employing Cu $K_{\alpha 1}$ radiation under the conditions 50 kV and 40 mA. The samples were scanned at 0.03° intervals of 2θ in the range 10–120°; the scan rate was 0.01° $2\theta\,s^{-1}$. Following identification of the peaks, Rietveld refinement was carried out using the Topas[23] refinement programme. The initial atomic coordinates for the NKN crystal structure were taken from Kumada et al. [24]

For microstructural examination, by scanning electron microscopy (SEM) (Jeol 6300 and Philips XL30, equipped with energy dispersive spectrometers (EDS) for chemical analysis), the sintered surface of the ceramics were first carbon coated. Selected samples were ground then polished down to 0.25 μm diamond paste followed by polishing with OPS (colloidal silica suspension) for 5 h, then chemically etched with hot sulphuric acid.

For dielectric and piezoelectric measurements, the disc shaped samples were ground on SiC paper to reduce the thickness to less than 1 mm and coated with silver paste. Dielectric constant, loss tangent and impedance were determined by use of an Impedance Analyser (HP 4192A) at frequencies of 10 Hz to 10 MHz; samples were heated from room temperature to 600 °C in a Carbolite (MTF 9/15/130) tube furnace. Polarization–electric field (*P–E*) hysteresis measurements were undertaken using a Sawyer-Tower circuit, with a high voltage amplifier, at 2 Hz with temperatures ranging from 25 °C to 150 °C.

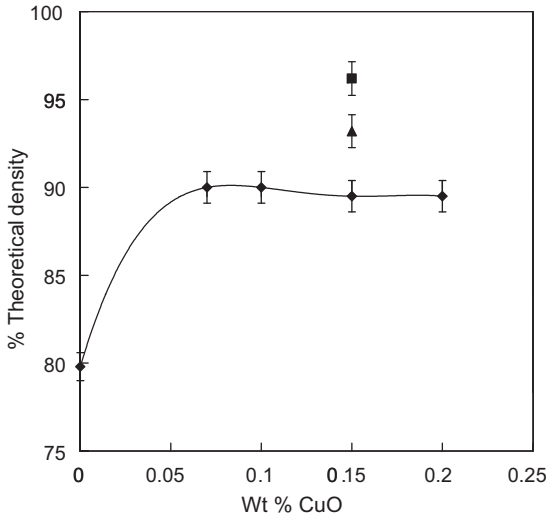

Fig. 1. The effect of CuO content and calcination temperature on the density of NKN ceramics: (♦) calcined at 850 °C, (■) calcined at 890 °C, (▲) calcined at 930 °C.

3. Results and discussion

3.1. Densification

It was difficult to densify the pure NKN ceramics; product densities were less than 4.0 g cm^{-3}, well below 90% of the theoretical density of NKN. Additions of CuO to the starting mixtures readily improved the density of the NKN ceramics. The final density was also sensitive to the calcination temperature. In earlier investigations, calcination temperatures ranging from 850 °C to 930 °C have been used.[4,13,15] In the present study, increasing the calcination temperature from 850 °C to 950 °C resulted in an almost linear increase in sintered density, achieving a maximum of 95% theoretical density for a calcination temperature of 930 °C and 0.15 wt% CuO (Fig. 1). For CuO doped NKN ceramics, the optimum sintering temperature was found to be 1090 °C. For the Li-bearing specimens, the effect of CuO additions on the densification behaviour of the NKN + 5 mole% $LiNbO_3$ (NKLN) is shown in Fig. 2. It was found that when lithium was present in the NKN formulation, the CuO additions significantly reduced the optimum sintering temperature. High density ceramics (95% of theoretical) could be obtained by sintering at 890 °C with up to 0.8 wt% CuO (Fig. 2). In both cases (with and without Li addition) the presence of CuO appears to enhance densification of NKN-based ceramics by a liquid phase mechanism.[15,25] This will be addressed in more detail in a later section.

3.2. X-ray diffraction analysis

X-ray diffraction (XRD) analysis of the base composition (NKN prepared with 0% CuO) confirmed an orthorhombic structure. In contrast, for the NKLN the Rietveld refinement revealed

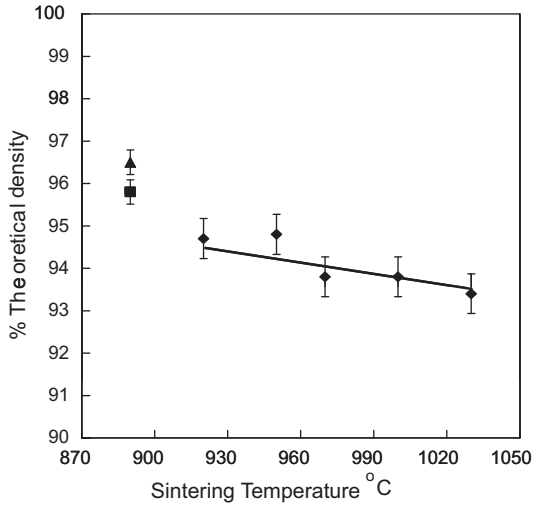

Fig. 2. The effect of sintering temperature and CuO content on the density of NKLN ceramics: (♦) NKLN + 0.2CuO, (■) NKLN + 0.4CuO, (▲) NKLN + 0.8CuO.

that two structures coexisted, orthorhombic and tetragonal; for example Fig. 3a shows the spectrum for NKLN + 0.4 wt% CuO, which has been indexed according to the data of Kumada et al.[24] Refinement of the spectrum for undoped NKLN showed 60% could be attributed to orthorhombic and the rest to the tetragonal phase. The CuO doped NKLN samples showed very similar XRD spectra, but there were changes in the peak positions and intensities. For example, Fig. 3b shows the changes in position of $(0\,1\,1)_{orthorhombic}$, $(1\,0\,0)_{orthorhombic}$, $(0\,0\,1)_{tetragonal}$ and $(0\,1\,0)_{tetragonal}$ peaks as a function of CuO additions to NKLN ceramics (with NKN data included for comparison purposes). The data show that for up to 0.2 wt% additions the NKLN peaks are displaced to lower angles, but for higher levels of CuO additions (up to 0.8 wt%) these peaks are actually displaced *back to higher angles*, towards the peak positions recorded for undoped NKLN. Since the ionic size of Cu^{2+} ($r_{Cu}{}^{2+}$:0.87 Å) is smaller than the size of the original A-site ions ($r_K{}^{1+}$:1.52 Å, $r_{Na}{}^{1+}$:1.16 Å, $r_{Li}{}^{1+}$:0.90 Å)[26] then the displacements of the peaks upon doping suggests that Cu initially enters the A site and then for the higher levels of CuO additions (0.2–0.8 wt%) it then enters the B-site. Accurate determinations of orthorhombic to tetragonal phase ratios and lattice parameters must await appropriate high resolution synchrotron radiation XRD investigations.

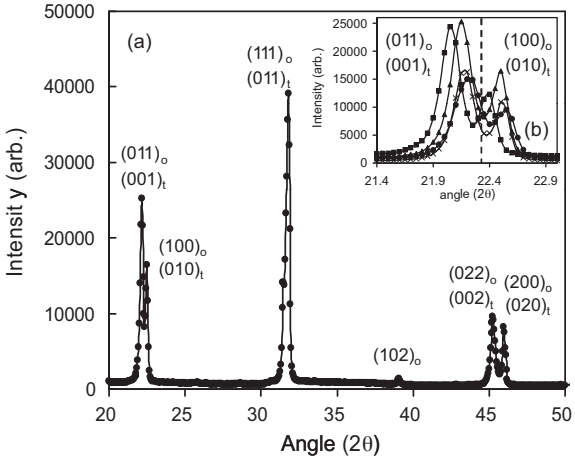

Fig. 3. XRD spectra of CuO doped NKN-based ceramics: (a) NKLN + 0.4 wt% CuO; (b) enlarged low angle spectra showing data for: (●) NKN, 9■) NKLN + 0.2CuO, (▲) NKLN + 0.4CuO, (×) NKLN + 0.8CuO (subscripts o and t on the indices for individual peaks refer to orthorhombic and tetragonal structures, respectively). The dashed vertical line in (b) has been inserted for clarity.

3.3. Microstructural analysis

SEM analysis of as-sintered surfaces, and polished and etched surfaces provided information about grain growth and domain structures in the ceramics. The low density, undoped specimens generally exhibited grain sizes in the range of ~5–30 μm with much evidence of abnormal grain growth. The additions of CuO aided microstructural development and tended to reduce abnormal grain growth. Fig. 4 shows SEM micrographs of polished and etched surfaces of an NKN + 0.2 wt% CuO sample sintered at 1090 °C for 4 h. The grain size varies between 2 μm and 15 μm (Fig. 4a). The higher magnification image of the same sample (Fig. 4b) shows herring-bone type and water mark type ferroelectric domains. The domain structure of the base material NKN is very similar to that of CuO-doped NKN prepared with low levels of CuO (0.075–0.2 wt%). Domain structure images would therefore be almost identical; for this reason they have been omitted. However the undoped material has very low density ~80% theoretical making it difficult to produce high quality samples and clear domain images.

In the context of NKN, having an orthorhombic structure, the primary direction of polarization is [1 1 0] and there are 12 possible directions of polarization. The angle between two polarization vectors can be 60°, 90°, 120° or 180°. The domain walls for 60° and 120° type domains are on (1 1 0) and the 90° type domains on (1 0 0). Consequently they all appear as lamellae. The 180° domain walls do not lie on specific atomic planes and therefore appear as cured boundaries. Using piezoelectric force microscopy (PFM), Cho et al.[27] identified the lamellar domains in their NKN based ceramics as 60°, 90° and 120° types; curved (180°) domains were also present.

Our NKLN and NKLN + 0.2 wt% CuO samples showed herring-bone and water mark type structures (Fig. 5a and b) as in the NKN + 0.2 wt% CuO. The NKLN + 0.4 wt% CuO and NKNLN + 0.8CuO samples showed different morphologies (Fig. 5c and,d). This suggests that CuO additions modify the domain structures in NKLN ceramics. The NKLN composition is at a morphotropic phase boundary (MPB). The microstructure should consist of 90° and 180° type domains for the tetragonal phase (for a tetragonal ferroelectric the direction of polarization is [0 0 1] and there are six direction of polarization and two possible 90° and 180° domains) and 60°, 90°, 120° and 180° type domains for the orthorhombic phase. Herber et al.[28] characterized the domains of a MPB phase of NKN modified by $Li(Nb,Ta,Sb)O_3$ substituted by PFM. They reported similar lamellar patterns as those present in our NKLN. Herber et al. found that the ferroelectric domains of the orthorhombic phase

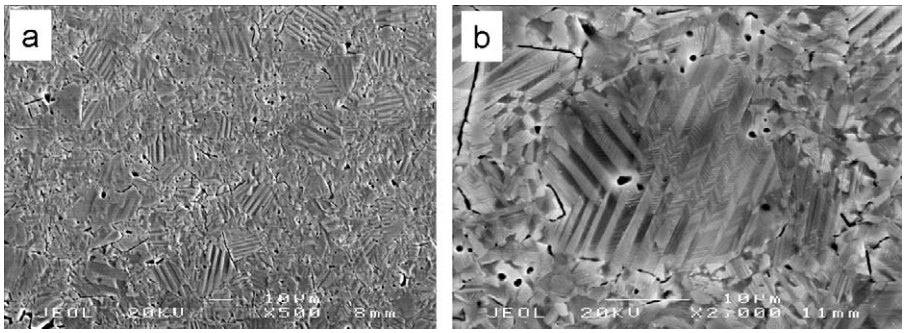

Fig. 4. SEM micrographs of the polished and etched surface of NKN + 0.2 wt% CuO showing (a) the distribution of domains and (b) high magnification image showing herring-bone type and water mark type ferroelectric domains.

and tetragonal phase coexist as adjacent layers separated by {1 1 0} planes.

When NKN is prepared with CuO additions a secondary phase develops at the grain boundaries. EDS analysis confirmed that this phase has a composition close to $K_4CuNb_8O_{23}$, as reported by other authors.[29,30] In the case of NKLN, a secondary phase was also formed at the grain boundaries (Fig. 6) as an extensive interconnecting network. EDS analysis revealed only Cu and O in the sample. However, since Li cannot be detected by EDS it is likely that the second phase which greatly lowered the sintering temperature of NKLN is essentially a eutectic phase between CuO and Li_2O since there four eutectic compositions in the CuO–Li_2O binary system[31] with the melting temperatures between 830 °C and 930 °C. As we successfully produced high density NKLN ceramics with a sintering temperature of 890 °C it seems likely that the eutectic was CuO and Li_6CuO_4 at about 16 mole% CuO which have eutectic temperature of 880 °C.

3.4. Dielectric properties

All NKN and NKLN samples showed broadly similar dielectric properties in terms of the temperature dependence of relative permittivity and loss tangent. With increasing temperature there were three clear regions, separated by firstly the orthorhombic–tetragonal phase transition and then the tetragonal–cubic phase transition. For undoped NKN the two transition temperatures (Fig. 7) were found at 220 °C and 420 °C, respectively. These values are consistent with previous studies

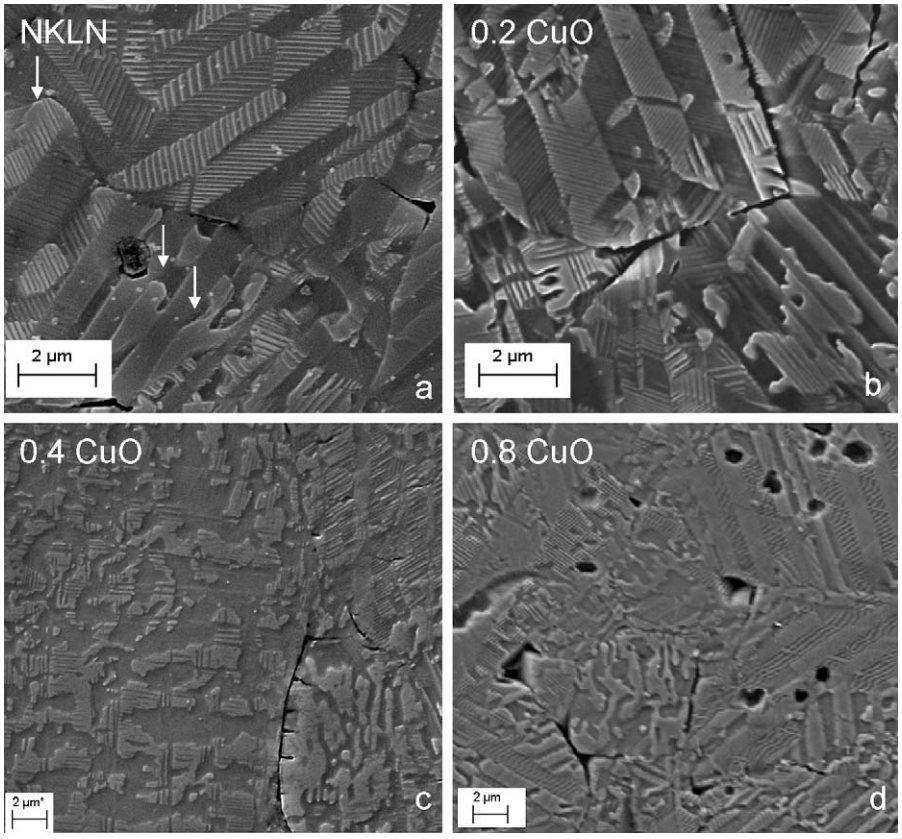

Fig. 5. Ferroelectric domain patterns for NKLN ceramics as function of CuO content: (a) 0.0 wt%, (b) 0.2 wt%, (c) 0.4, wt% and (d) 0.8 wt%.

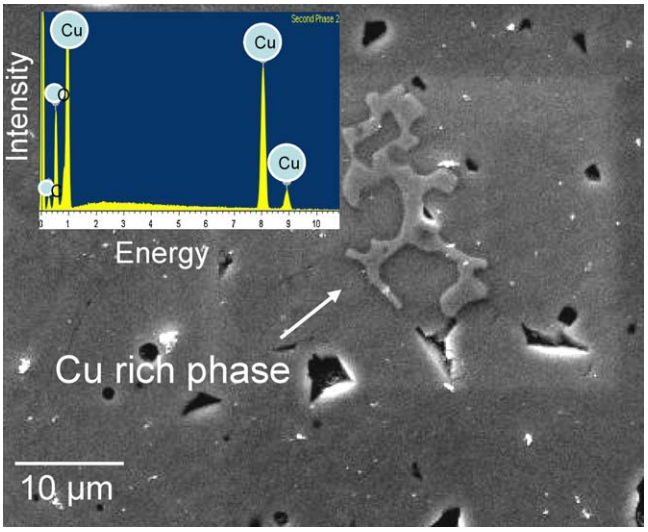

Fig. 6. SEM image and EDS spectra of the Cu-rich second phase in NKLN + 0.4 wt% CuO sintered at 920 °C.

of NKN.[3,12,13] The transition temperatures do not change upon the addition of CuO (up to 0.2 wt%), in agreement with the findings of for example Park et al.,[32] but increasing additions of Cu increased the relative permittivity at the tetragonal to cubic phase transition (T_C). This increase is possibly due to the higher density of the doped NKN (Fig. 1) rather than the substitution of low levels of Cu in the NKN lattice.

Introduction of $LiNbO_3$ into NKN, even at the 5% level, caused the orthorhombic/tetragonal transition temperature to be reduced by approximately 100 °C, the tetragonal/cubic transition temperature to be increased by about 50 °C, and the relative permittivity to be reduced at all temperatures (Fig. 7). These trends are in agreement with the data reported by Guo et al.[22] and Higashide et al.[33] However, Hagh et al. [30] found that additions of $LiTaO_3$ and $LiSbO_3$ to NKN caused both transition temperatures to be reduced by approximately 150 °C (the orthorhombic/tetragonal to 34 °C and tetragonal/cubic to 264 °C), thus bringing the orthorhombic–tetragonal transition close to room temperature. The addition of CuO to NKLN slightly reduced the relative permittivity (Fig. 7), in agreement

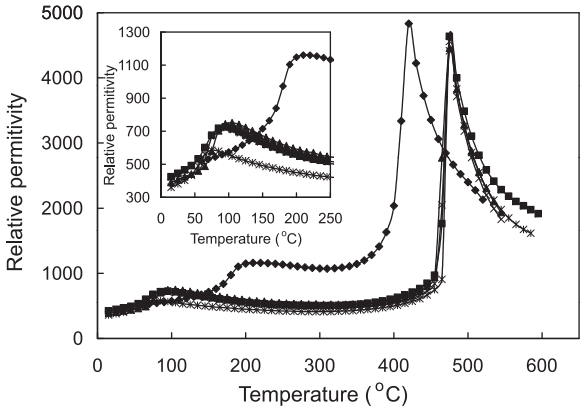

Fig. 7. Temperature dependence of relative permittivity of NKN and NKLN ceramics: (♦) NKN + 0.2CuO, (■) NKN + 5LN, (▲) NKN + 5LN + 0.2CuO, (×) NKN + 5LN + 0.4CuO, (*) NKN + 5LN + 0.8CuO.

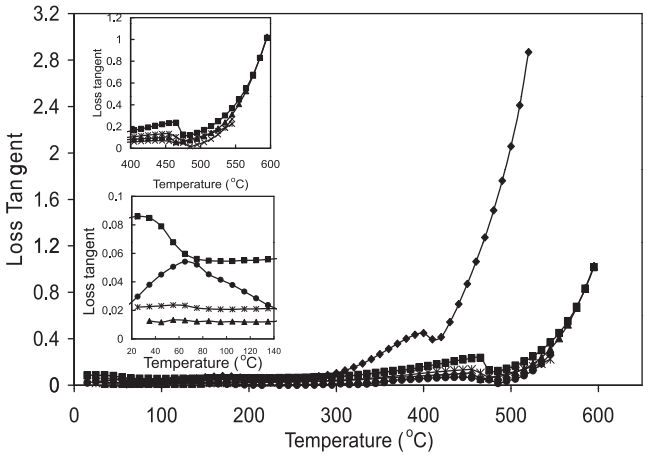

Fig. 8. Temperature dependence of dielectric loss for NKN and NKLN ceramics: (♦) NKN + 0.2CuO, (■) NKN + 5LN, (▲) NKN + 5LN + 0.2CuO, (×) NKN + 5LN + 0.4CuO, (*) NKN + 5LN + 0.8CuO.

with studies of a range of Cu doped alkali niobate systems, where there was a distinct lowering of ε_r, especially at the Curie point.[30,34,35] Most investigations of the alkali niobate systems have found the tetragonal to cubic Curie temperature to be insensitive to additions of Cu.[30,34,35] A rare exception was Li et al.[29] who reported a small change in the Curie temperature (~4 °C) at the level of 0.3 wt% Cu additions. In agreement with Lin et al.[35] and Hagh et al.[30] we did not observe a significant change in the orthorhombic–tetragonal Curie temperature, except at the very highest doping levels, where the T_{o-t} was displaced to lower temperatures, possibly suggesting that Cu additions stabilise the tetragonal phase. In the dielectric loss data (Fig. 8), it is clear that the substitution of 5 mole% $LiNbO_3$ into NKN led to a sharp reduction in the dielectric loss around the transition temperatures and the subsequent addition of Cu significantly reduced the dielectric loss of NKLN from room temperature to above the Curie temperatures. Although 5 mole% substitution of $LiNbO_3$ into NKN has considerably lowered the orthorhombic to tetragonal phase transition to ~80 °C when there is added Cu, the XRD data confirms that there is still a significant fraction of orthorhombic phase present. To achieve full conversion to tetragonal phase near room temperature would require much more than 5 mole% substitution of $LiNbO_3$ into NKN.

3.5. Piezoelectric properties

Undoped NKN samples showed high dielectric loss and high coercive field (E_c) values; it was difficult to apply electric fields greater than 2 kV/mm without breakdown occurring. Fig. 9a shows the room temperature polarization–hysteresis (P–E) loop for NKN ceramics prepared with 0.2 wt% CuO additions, sintered at 1090 °C for 4 h. There was comparatively little difference for samples sintered up to 12 h. The additions reduced dielectric loss and E_c; electric fields up to 4 kV/mm could readily be applied to the samples (Fig. 9a). Typically the samples exhibited P_r and E_c values of 0.18 C/m^{-2} and 1.5 kV/mm, respectively, which are comparable with the best published data for CuO doped NKN ceramics.[15,29,36] Similar

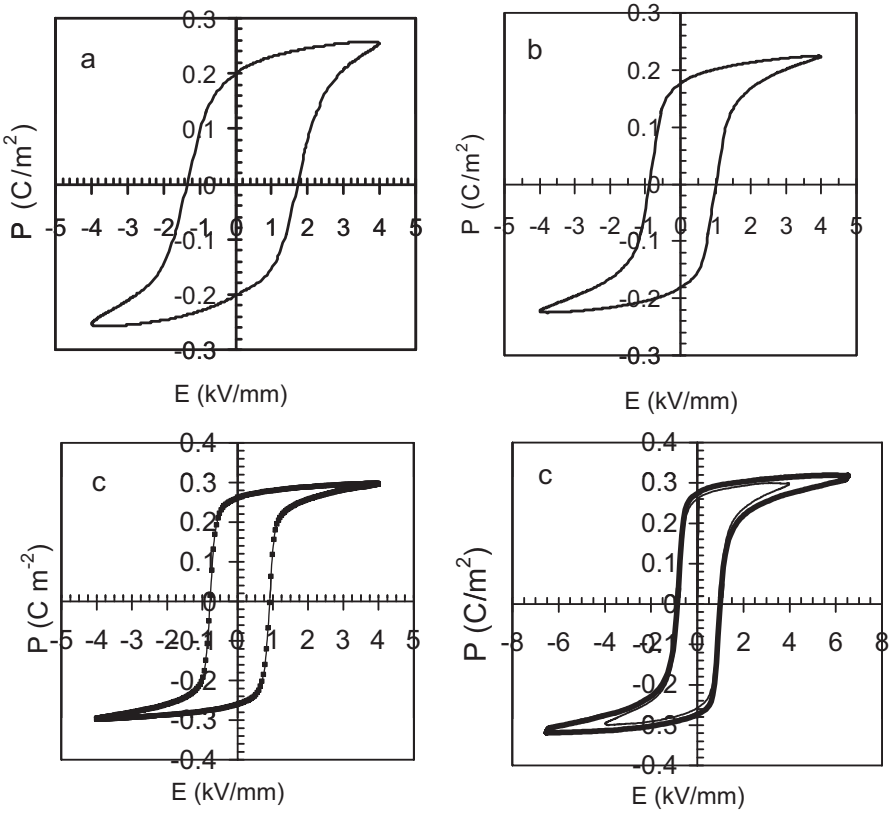

Fig. 9. Polarization–electric field response of NKN- and NKLN-based ceramics: (a) NKN + 0.2CuO sintered for 4 h, (b) NKLN + 0.2CuO sintered at 920 °C, (c) NKLN + 0.4CuO sintered at 890 °C, (d) NKLN + 0.8 CuO sintered at 890 °C; data collected at 4 kV/mm (feint line) and data collected at 7 kV/mm (bold line).

polarization–electric field (*P–E*) responses were observed for the NKLN ceramics. Samples prepared with additions of CuO exhibited well saturated *P–E* loops with reduced hysteresis loop areas, brought about by the reduction of E_c and increase P_r as shown in Fig. 9b–d. The *P–E* response of CuO added NKLN was insensitive to the sintering temperature range of 920–1000 °C (Fig. 9b shows data for samples sintered at 920 °C). For NKLN samples sintered at the lowest temperature of 890 °C the E_c reduced to less than 1 kV/mm and the saturation polarization characteristics sharpened further (Fig. 9c). As the CuO additions were increased to 0.8 wt% the breakdown field increased to a maximum of 8.0 kV/mm (Fig. 8d). The highest value achieved for P_r was 0.28 C/mm^{-2}, and this was by the use of 0.4 wt% additions of CuO.

In both NKN and NKLN ceramics the addition of CuO to the starting formulation improved densification by generation of the $K_4CuNb_8O_{23}$ and (Li–Cu) rich secondary phases, respectively (which in turn enabled lower sintering temperatures), and improved dielectric and piezoelectric properties. Park et al.,[32] working on NKN prepared with ZnO and CuO additions, attributed the superior piezoelectric properties to the hardening effect of Cu^{2+} ions.[16] If this is correct then it would be expected that Cu would be incorporated into the perovskite structure. If Cu enters the A site, then copper (a 2+ ion) replacing Na or K or Li (1+ ions) would act as a donor. On the basis of simple Kroger-Vink analysis Hagh et al.[30] argued that this would give rise to A site vacancies to achieve charge balance. In contrast, for Cu entering the smaller octahedral B site in place of Nb, Hagh et al.[30] suggested that oxygen vacancies would be generated. In this way they proposed that the hardening of their NKN–$LiTaO_3$–$LiSbO_3$ ceramics was caused by the generation of oxygen vacancies. Such a mechanism is also consistent with the present dielectric loss data for NKN and NKLN ceramics, where additions of CuO led to a reduction of the dielectric loss. However, Hagh et al.[30] noted that the anticipated increase in coercive field (E_c) did not occur on Cu doping and therefore concluded that Cu probably entered both the A- and B-sites of the perovskite structure. This had been suggested earlier by Li et al.[29] on the basis of the change of lattice volume as a function of CuO additions. They suggested that at low levels of doping, the Cu^{2+} is incorporated in the A-site and then at higher levels it substitutes in both sites. Our XRD data (Fig. 3), for the movement of the (0 0 1) and (1 1 0) peaks upon doping would support the model of Li et al.[29] An additional effect of the incorporation of Cu into the structure could be domain wall stabilisation. Park et al.[32] suggested that the substitution of Cu causes the piezoelectric hardening of NKN and a side effect is the pinning of domain walls by the increased population of oxygen vacancies, thereby stabilising the domain walls; this in turn is manifest by an improved mechanical *Q* value. There is very little direct evidence of site occupancies for additives in piezoelectric materials. However a recent study Eichel et al.[37] found evidence of Cu^{2+} behaving as acceptors, entering the B sites of both PZT and NKN.

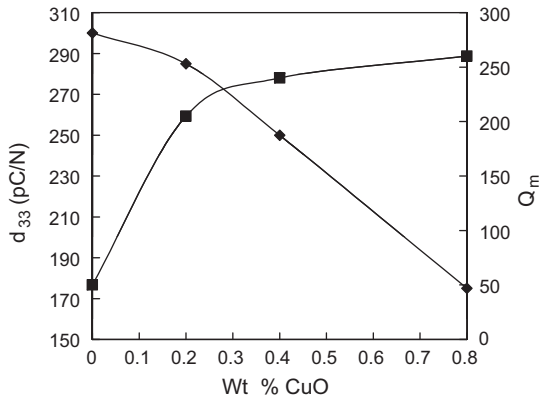

Fig. 10. The effect of CuO content on the d_{33} (♦) and Q_m (■) values of NKLN ceramics.

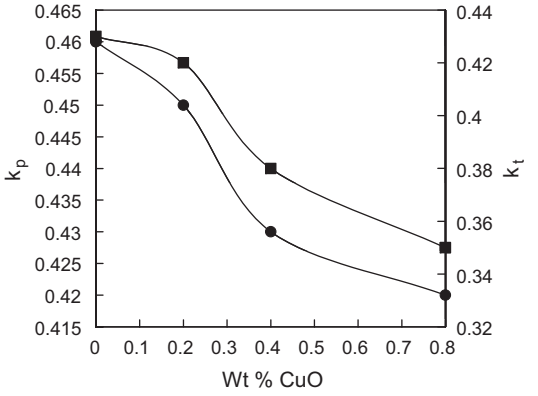

Fig. 11. The effect of CuO content on the coupling factors k_p (●) and k_t (■) of NKLN ceramics.

Fig. 10 shows the effect of CuO additions on the d_{33} and Q_m of NKLN ceramics. There is a remarkable increase in Q_m from 50 to 260. The hardening of NKN based ceramics upon additions of CuO has been reported for a number of systems.[16,30,35] In addition to lowering the sintering temperature and improving densification, the hardening or improvement in Q_m is one of the main benefits of CuO additions. In contrast the d_{33} values decreased with CuO additions (Fig. 10). For NKLN ceramics prepared with 0.2–0.4 wt% CuO, both Q_m and d_{33} values are reasonably high. The main extrinsic contribution to the dielectric and piezoelectric properties of ferroelectric ceramics is domain wall motions.[38] We have shown that CuO additions modify the domain structure (Fig. 6). Although it has not been quantified it is probable that the modification alters the density of different type of domains and this in turn affects the Q_m. The incorporation of Cu ions as acceptor dopants also act to reduce the dielectric and mechanical losses through domain pinning as discussed above. Finally, Fig. 11 shows the effect of CuO additions on the coupling factors k_p and k_t for NKLN ceramics. Both parameters reduce as CuO is added but the reduction is minimal at 0.2 wt% CuO. At this level of doping both d_{33} and Q_m are also acceptably high (Fig. 10), pointing the way for a particularly useful formulation.

4. Conclusions

The addition copper oxide to $Na_{0.5}K_{0.5}NbO_3$ (NKN) and $Na_{0.475}K_{0.475}Li_{0.05}NbO_3$ (NKLN) improved densification of the ceramics (to over 96% theoretical) and reduced the sintering temperature to below 900 °C by a liquid phase mechanism, giving rise to a second phase in NKN of $K_4CuNb_8O_{23}$.

NKN prepared without CuO exhibited an orthorhombic structure, whilst in NKLN two structures coexisted, orthorhombic and tetragonal. In undoped NKLN the relative proportions were approximately 60% orthorhombic and 40% tetragonal phase. Displacements of the XRD peaks upon doping suggests that Cu initially enters the A site and then at higher levels (0.2–0.8 wt% CuO additions) it enters the B-site.

The use of CuO additions aided microstructure development, reducing abnormal grain growth giving grain sizes in the range 2–15 μm in NKN. Domain structures were of the lamellar type and water mark type for NKN and NKLN, respectively. The size and distribution of the domains were affected by Cu content.

In NKN ceramics the orthorhombic–tetragonal and tetragonal–cubic phase transitions occurred at temperatures of approximately 225 °C and 410 °C, respectively. The introduction of $LiNbO_3$ into NKN, even at the 5% level, caused the orthorhombic/tetragonal transition temperature to be reduced by approximately 150 °C, the tetragonal/cubic transition temperature to be increased by about 50 °C, and the relative permittivity to be reduced at all temperatures.

CuO doped NKN and NKLN ceramics retain strong ferroelectricity, with an increase in remanent polarization and decrease coercive field with the amount of additive. For example, NKLN prepared with 0.4 wt% CuO sintered at 890 °C exhibited a saturation polarization (P_{sat}) of 0.30 C/m^2, remanent polarization of 0.27 C/m^2 and coercive electric field of 1.0 kV/mm. Increasing the CuO to 0.8 wt% raised the breakdown field to a maximum of 8.0 kV/mm. As CuO was added to NKLN the ceramics hardened considerably, Q_m increased from 50 to 220 and the other piezoelectric properties remained consistently high ($d_{33} = 285$, $k_p = 0.42$ and $k_t = 0.45$).

Acknowledgements

We would like to acknowledge the support from EPSRC through award GR/T19148 and the provision of a Doctoral Training award to M Wegryzn. The award of a British Council UKIERI Fellowship to S Sharma is gratefully acknowledged.

References

1. Tressler JF, Alkroy S, Newnham RE. Piezoelectric sensors and sensor materials. *J Electroceram* 1998;**2**:257–72.
2. European Union, Restriction of Hazardous substances (RoHS), Directive 2002/95/EC; and 2008/34/EC on Waste Electrical and Electronic Equipment (WEEE).
3. Shirane G, Newnham R, Pepinsky R. Dielectric properties and phase transitions of $NaNbO_3$ and $(Na,K)NbO_3$. *Phys Rev* 1954;**96**:581–8.
4. Kakimoto K, Higashide K, Hotta T, Ohsato H. Temperature dependence on the structure and property of $Li_{0.06}(Na_{0.5}K_{0.5})_{(0.94)}NbO_3$ piezoceramics. *Adv Electron Ceram* 2008;**28**:25–31.

5. Abe J, Kobune M, Kitada K, Yazawa T, Masumoto H, Goto T. Effects of spark-plasma sintering on the piezoelectric properties of high-density $(1-x)(Na_{0.5}K_{0.5})NbO_3$–$x$$LiTaO_3$ ceramics. *J Korean Phys Soc* 2007;**51**:810–4.
6. Dunmin L, Kwok KW, Lam KH, Chan HLW. Structure and electrical properties of $K_{0.5}Na_{0.5}NbO_3$–$LiSbO_3$ lead-free piezoelectric ceramics. *J Appl Phys* 2007;**101**:074111.
7. Park H-Y, Cho K-H, Paik D-S, Nahm S. Microstructure and piezoelectric properties of lead-free $(1-x)Na_{0.5}K_{0.5}NbO_3$–$x$$CaTiO_3$ ceramics. *J Appl Phys* 2007;**102**:124101.
8. Guo Y, Kakimoto K, Ohsato H. Dielectric and piezoelectric properties of lead-free $(Na_{0.5}K_{0.5})NbO_3$–$SrTiO_3$ ceramics. *Solid State Commun* 2004;**129**:279–84.
9. Zuo R, Ye C, Fang X. $Na_{0.5}K_{0.5}NbO_3$–$BiScO_3$ lead-free piezoelectric ceramics. *Jpn J Appl Phys* 2007;**46**:6733–6.
10. Zuo R, Ye C, Fang X. $Na_{0.5}K_{0.5}NbO_3$–$BiFeO_3$ lead-free piezoelectric ceramics. *J Phys Chem Solids* 2008;**69**:230–5.
11. Guo Y, Kakimoto K, Ohsato H. Structure and electrical properties of lead-free $Na_{0.5}K_{0.5}NbO_3$–$BaTiO_3$ ceramics. *Jpn J Appl Phys* 2004;**43**:6662–6.
12. Jeager RE, Egerton L. Hot pressing of potassium–sodium niobate. *J Am Ceram Soc* 1962;**45**:208–13.
13. Zuo R, Rodel JR, Chen R, Li L. Sintering and electrical properties of lead-free $Na_{0.5}K_{0.5}NbO_3$ piezoelectric ceramics. *J Am Ceram Soc* 2006;**89**:2010–5.
14. Wang R, Xie R, Sekiya T, Shimojo Y. Fabrication and characterization of potassium–sodium niobate piezoelectric ceramics by spark-plasma-sintering method. *Mater Res Bull* 2004;**39**:1709–15.
15. Park S-H, Ahn C-W, Nahm S, Song J-S. Microstructure and piezoelectric properties of ZnO-added $(Na_{0.5}K_{0.5})NbO_3$ ceramics. *Jpn J Appl Phys* 2004;**43**:L1072–4.
16. Park HY, Ahn CW, Cho KH, Nahm S, Lee HG, Kang HW, et al. Low-temperature sintering and piezoelectric properties of CuO-added $0.95(Na_{0.5}K_{0.5}NbO_3)$–$0.05BaTiO_3$ ceramics. *J Am Ceram Soc* 2007;**90**:4066–9.
17. Park HY, Choi JY, Choi MK, Cho K-H, Nahm S, Lee H-G, et al. Microstructure and piezoelectric properties of the CuO added $(Na_{0.5}K_{0.5})NbO_3$ lead-free piezoelectric ceramics. *J Appl Phys* 2008;**104**:034103.
18. Seo IT, Park HY, Van Dung N, Choi MK, Nahm S, Lee HG. Microstructure and piezoelectric properties of $(Na_{0.5}K_{0.5})NbO_3$ lead-free piezoelectric ceramics with V_2O_5 addition. *IEEE Trans Ultranson Ferroelectr Freq Control* 2009;**56**:2337–42.
19. Lin D, Kwok KW, Chan HLW. Piezoelectric and ferroelectric properties of $K_xNa_{1-x}NbO_3$ lead-free ceramics with MnO_2 and CuO doping. *J Alloys Compd* 2008;**461**:273–8.
20. Saito Y, Takao H, Tani T, Nanoyama T, Takatori K, Homma T, et al. Lead-free piezoceramics. *Nature* 2004;**123**:84–7.
21. Zou R, Su S, Fu J, Xu Z. Structures and electric properties of $(Na_{0.5}K_{0.5})NbO_3$–$Li(Ta_{0.5}Nb_{0.5})O_3$ piezoelectric ceramics. *J Mater Sci Electron Mater* 2009;**20**:469–72.
22. Guo YP, Kakimoto K, Ohsato H. Phase transitional behaviour and piezoelectric properties of $(Na_{0.5}K_{0.5})NbO_3$–$LiNbO_3$ ceramics. *Appl Phys Lett* 2004;**85**:4121–4.
23. TOPAS software (Ver. 2.1). Bruker AXS Ltd., Coventry, U.K. (2003).
24. Kumada N, Kyoda T, Yonesaki Y, Takei T, Kinomura N. Preparation of $KNbO_3$ by hydrothermal reaction. *Mater Res Bull* 2007;**42**:1856–62.
25. Matsubara M, Yamaguchi T, Sakamoto W, Kikata K, Yogo T, Hirano S-I. Processing and piezoelectric properties of lead-free $(K,Na)(Nb,Ta)O_3$ ceramics. *J Am Ceram Soc* 2005;**88**:1190–6.
26. Shannon RD. Revised effective ionic radii and systematic studies of interatomic distances in halides and chalcogenides. *Acta Crystallogr* 1976;**A32**:751–67.
27. Cho YH, Lee YH, Kan KS, Chun MP, Nam JH, Kim BI. Grain size effect on domain structure of KNN-based ceramics. In: *Poster C-P-19, ECerS Conference*. 2009.
28. Herber R-F, Schneider GA, Wanger S, Hoffmann MJ. Characterization of ferroelectric domains in morphotropic potassium sodium niobate with scanning probe microscopy. *Appl Phys Lett* 2007;**90**:252905.
29. Li E, Kakimoto H, Wada S, Tsurumi T. Influence of CuO on the structure and piezoelectric properties of alkaline niobate-based lead-free ceramics. *J Am Ceram Soc* 2007;**90**:1787–91.
30. Hagh NM, Kerman K, Jadidian B, Safari A. Dielectric and piezoelectric properties of Cu^{2+} doped alkali niobates. *J Eur Ceram Soc* 2009;**29**:2325–32.
31. Abdullaevn GK, Rza-Zade PF, Mamedov KS. System Li_2O–CuO. *Russ J Inorg Chem (Engl Transl)* 1982;**27**:1037–40.
32. Park H-Y, Seo I-T, Choi J-H, Nahm S, Lee H-G. Low temperature sintering and piezoelectric properties of $(Na_{0.5}K_{0.5})NbO_3$ lead-free piezoelectric ceramics. *J Am Ceram Soc* 2009;**91**:36–9.
33. Higashide K, Kakimoto K, Ohsato H. Temperature dependence on piezoelectric properties of $(1-x)(Na_{0.5}K_{0.5})NbO_3$–$x$$LiNbO_3$ ceramics. *J Eur Ceram Soc* 2007;**27**:4107–10.
34. Takao H, Saito Y, Aoki Y, Horibuchi K. Microstructure evolution of crystalline-oriented $(K_{0.5}Na_{0.5})NbO_3$ piezoelectric ceramics with a sintering aid of CuO. *J Am Ceram Soc* 2006;**89**:1951–6.
35. Lin D, Kwok KW, Chan HLW. Double hysteresis loops in Cu-doped $K_{0.5}Na_{0.5}NbO_3$ lead-free piezoelectric ceramics. *Appl Phys Lett* 2007;**90**:232903.
36. Chen Q, Chen L, Li Q, Yue X, Xiao D, Zhu J. Piezoelectric properties of $K_4CuNb_8O_{23}$ modified $(Na_{0.5}K_{0.5})NbO_3$ lead-free piezoceramics. *J Appl Phys* 2007;**102**:104109.
37. Eichel R-A, Erunal E, Drahus MD, Smyth DM, van Tol J, Acker J, et al. Local variations in defect polarization and covalent bonding in ferroelectric Cu(2+)-doped PZT and KNN functional ceramics at the morphotropic phase boundary. *Phys Chem Chem Phys* 2009;**11**:8698–705.
38. Herbiet R, Robels U, Hederichs H, Arlt G. Domain wall and volume contributions to material properties of PZT ceramics. *Ferroelectrics* 1998;**98**:107–21.